



HAL
open science

Dynamics of Full Fusion During Vesicular Exocytotic Events: Release of Adrenaline by Chromaffin Cells

Christian Amatore, Stéphane Arbault, Imelda Bonifas, Yann Bouret, Marie Erard, Manon Guille

► **To cite this version:**

Christian Amatore, Stéphane Arbault, Imelda Bonifas, Yann Bouret, Marie Erard, et al.. Dynamics of Full Fusion During Vesicular Exocytotic Events: Release of Adrenaline by Chromaffin Cells. ChemPhysChem, 2003, Electrochemistry, 4 (2), pp.147-154. 10.1002/cphc.200390024 . hal-04467881

HAL Id: hal-04467881

<https://hal.science/hal-04467881>

Submitted on 20 Feb 2024

HAL is a multi-disciplinary open access archive for the deposit and dissemination of scientific research documents, whether they are published or not. The documents may come from teaching and research institutions in France or abroad, or from public or private research centers.

L'archive ouverte pluridisciplinaire **HAL**, est destinée au dépôt et à la diffusion de documents scientifiques de niveau recherche, publiés ou non, émanant des établissements d'enseignement et de recherche français ou étrangers, des laboratoires publics ou privés.

**DYNAMICS OF FULL FUSION DURING VESICULAR EXOCYTOTIC EVENTS:
RELEASE OF ADRENALINE BY CHROMAFFIN CELLS.**

Christian Amatore,^{*} Stéphane Arbault, Imelda Bonifas, Yann Bourret,
Marie Erard and Manon Guille.

*Département de Chimie, UMR CNRS-ENS-UPMC 8640 « PASTEUR », Ecole Normale Supérieure
24 rue Lhomond, 75231 PARIS Cedex 05. FRANCE*

Introduction

Vesicular exocytosis is a central feature in many processes of communication between living cells in complex organisms. This controls kinetically and thermodynamically the release of specific chemical or biochemical messengers (here neurotransmitters) stored in the emitting cell, which elicit specific response following their selective detection by the target receiving cells. This process is particularly crucial in synaptic transmission in the brain, in neuromuscular junctions and in controlling hormonal fluxes in blood.^[1-3]

Neurotransmitters are enclosed into vesicles stored inside the emitting cell (Figure 1). The vesicles generated by the reticulum endoplasmic and Golgi apparatus are packed within a membrane analogue to the cell cytoplasmic membrane. At the pH inside dense core vesicles, neurotransmitters such as catecholamines are cationic molecules and may thus be stored at high concentrations through multiple interactions such as hydrogen bonds and electrostatic interactions with a proteic polyanionic matrix which fills the inside of vesicles. Following the cell stimulation, in our case bovine chromaffin cells from adrenal glands involved in the control of adrenaline fluxes, the vesicles primed to secrete their content dock to determined loci of the internal cell membrane (phase I, Figure 2).^[2, 4] A protein machinery (SNAREs complex) is supposed to bring the vesicle membrane and the cell membrane in close contact so as to induce the formation of a transitory connection, the fusion pore.^[5-7] This nanometric pore connects the internal compartment of the vesicle and the external compartment of the cell (phase II, Figure 2). Based on electrochemical measurements of adrenaline diffusion

^{*} Corresponding author: Pr. C. Amatore. Fax : 33-1-4432-3863 ; e-mail: Christian.Amatore@ens.fr

through this fusion pore, its mean radius is estimated at about 1.5 nm, a value which is in agreement with that, 2 ± 1 nm, determined by patch-clamp techniques.^[8, 9] The structure of the pore is still a matter of a large debate. However, it has been shown that it may become unstable and enlarge suddenly to lead to the complete fusion of the vesicle and cell membranes (phase III, Figure 2). At the end of phase III, the former vesicle matrix is fully exposed to the extracellular fluid and release of neurotransmitters is pursued through simple diffusion (phase IV). These four different phases were previously identified by patch-clamp^[10, 11] and evanescent field fluorescent spectroscopy techniques,^[12, 13] however the kinetic resolutions of these methods were too low to analyze precisely the transition between phase II and III or to monitor accurately the dynamics of events during phases III and IV. Because of the lack of precise kinetic informations on these central events, the nature of the physicochemical events which concurred to their existence have long remained highly speculative and controversial.

Electrochemical measurements of the rate of neurotransmitters secretion with ultramicroelectrodes allowed to quantify these events with the precision required to propose and validate soundly physicochemical models that might rationalize their occurrence.^[14, 15] The precise positioning of an ultramicroelectrode at micrometric distances from an isolated living cell (neuron, chromaffin, mast or pancreatic cell, fibroblast, macrophage ...)^[3, 16, 17] ensures that selected electroactive material released by the cell can be collected and analyzed by the electrode surface (Figure 3a), reflecting precisely the cellular release kinetics. Indeed, the film of extracellular fluid comprised between the cell and the electrode surfaces defines an artificial synaptic cleft of a few hundred femtoliters volume, in which the release of minute molecular amounts of chemicals, typically in the range of zepto- to attomoles, produces a sudden and significant concentration rise. This guarantees the detection of the released species with an extremely high signal-to-noise ratio, as well as the determination of the instant released fluxes since the collection efficiency is quantitative. In other words, the assembly cell / liquid cleft / ultramicroelectrode behaves as an artificial synapse and the ultramicroelectrode current mirrors precisely the released fluxes (Figure 3b,c).

Based on this artificial synapse method, carbon fiber ultramicroelectrodes were used to monitor the kinetics of exocytosis of adrenaline by bovine chromaffin cells (Figure 3). Adrenaline molecules that diffuse away from the cell are electrooxidized (two electrons per molecule^[18]) at the surface of the ultramicroelectrode and their flux, $dN(t)/dt$, where $N(t)$ is the number of catecholamine molecules emitted at the time t , is converted

electrochemically into a current $I(t)$ according to the Faraday's law: $I(t) = 2F [dN(t)/dt]$, where F is the Faraday. The variation of the current with time is thus a precise kinetic measurement of the catecholamine efflux with a precision in the range of one thousand of molecules per millisecond (Figure 3b).

Such an extreme resolution offered a set of sufficiently precise kinetic data to elaborate and test a simple physico-chemical model to accurately describe the dynamics of vesicular exocytosis.^[15, 19] This model has established the determining role of the polyelectrolytic vesicular matrix on these events. In this view, the matrix is an active engine for the phenomenon and not only a suitable mean for tight and stable packaging of catecholamine cations at high concentrations (0.6 M on the average in chromaffin cells).^[20-22] Indeed, as soon phase II initiates, *viz.*, whenever the fusion pore opens, the concentration gradient of adrenaline monocations provokes their outward diffusion which, owing to electroneutrality, is compensated by the one-to-one entry of hydrated cations present in the external solution (Na^+ , H^+ , *etc.*). Replacement of catecholamine cations by the latter ones generates repulsive interactions within the matrix and induces its swelling.^[23, 24] This allows a local increase of diffusivities and further penetration of solvated ions, eventually leading to a cascade of released catecholamine molecules.

The constant transmitter flux through the fusion pore affords a steady-state low amperometric current of a few picoamperes (phase II, Figures 2, 3c). By comparison to current produced by an ultramicroelectrode this affords an estimate of the mean radius R_{pore} of the initial fusion pore at 1.5 nm as mentioned above.^[19] During this phase, the stability of the fusion pore, *viz.*, the overall constancy of its radius requires the presence of a specific structure which may be imposed by a biological architecture, *viz.*, protein(s), or by a specific heterogeneity among the bilipids present in the membrane. Our data, with their present resolution did not allow to discuss these matters which are still the source of important debates.^[25-27] However, it is clear that whatever the nanoscopic structure of the fusion pore is, at the physicochemical level, its energy is necessary controlled by two conflicting phenomena. One energy is positive and is related to the edge energy of the pore. It represents the increased energy of the bilipids located on the pore rim with respect to those within the membrane bulk. This energy acts to close the pore whenever it tends to open, and is by definition proportional to the length of the pore rim, *viz.*, $2\pi R_{\text{pore}}$. The second energy is negative and stems from Laplace tensions of the cell and vesicle membranes; it is then proportional to the surface area of the pore, *viz.*, πR_{pore}^2 . Thus, whenever the fusion pore radius fluctuates to enlarge ($R > R_{\text{pore}}$) its variation of energy is given by:

$$(dW_{\text{pore}}/dR)_{R \geq R_{\text{pore}}} = 2\pi[\rho - (\sigma_v + \sigma_c)R] \quad (1)$$

where ρ is the line energy coefficient of the pore edge; σ_v and σ_c are the surface tensions of the vesicle and the cell membrane, respectively. Note that in the above equation, the curvature of the cell and vesicle membranes are neglected due to the infinitely small size of the fusion pore radius (2 ± 1 nm) *vis a vis* those of the vesicle (150 nm) or of the cell (10 μ m). This shows that provided that the cumulated surface tension coefficients of the two membranes is lesser than a threshold value equal to (ρ/R_{pore}) , any fluctuation of the pore above its stable radius is immediately counteracted, *viz.*, $(dW_{\text{pore}}/dR) > 0$, so that it returns to its stable configuration at $R = R_{\text{pore}}$. Nonetheless, while the pore is opened, catecholamines are continuously exchanged, so that the matrix is altered near the pore entrance and tends to swell. However, any significant swelling of the matrix is then impeded owing to its constriction by the vesicle membrane, so that the energy resulting from the local alteration provokes an increase of the internal pressure within the vesicle. Owing to Laplace law, this increased pressure is compensated by an increased tension of the membrane, so that σ_v increases continuously while the fusion pore remains open. This shows that provided that the vesicle is large enough, the surface tension must ineluctably increase so as to reach the point where it compensates the edge energy of the pore, *viz.*, when $(\sigma_v + \sigma_c) = (\rho/R_{\text{pore}})$. Above this threshold value, any stochastic increase of the pore radius, provokes its irreversible enlargement since $(dW_{\text{pore}}/dR)_{R \geq R_{\text{pore}}}$ in eqn. (1) is negative when $(\sigma_v + \sigma_c) > (\rho/R_{\text{pore}})$. This provokes the irreversible resorption of the vesicle membrane through its continuous incorporation into the cell membrane. This initiates the beginning of phase *III* in Figure 2 and is reflected by a sharp increase of the current observed at the electrode in Figure 3c.

Phenomenologically, the spike shape of the time-course of adrenaline release may be well described by a skewed gaussian (see Figure 4), *viz.*, by a gaussian curve convoluted by an exponential.^[28] Therefore, such kinetics can not be determined by the rate of the matrix swelling. In fact, the rate determining phenomenon is the rate at which the vesicle membrane is incorporated into the cell membrane filtered by the diffusion rate of catecholamines out of the swollen matrix through its exposed area (Figure 2, *III*).^[14,19] Both processes are powered by the swelling of the intravesicular matrix but the rate of swelling does not limit the kinetics of release. This was confirmed quantitatively through the extraction from the chronoamperometric measurements of the variations of the fractional area of the spherical vesicle matrix of radius R_{vesicle} (see $a(t)$ in Figure 4)^[14] exposed to the extracellular fluid at time t after the beginning of the full-fusion event. In agreement with patch-clamp capacitance measurements,^[9, 11, 13] $a(t)$ has approximately a sigmoidal shape. However, the present precision evidences that $a(t)$ exhibits a profound asymmetry between the initial and the final phase of its time-course

(Figure 4). During the first period, *viz.*, before the diametral area of the vesicle is exposed, $a(t)$ increases explosively (Figure 4 insets), while it increases with a much smoother pace during the second phase. Such a dichotomic behavior reveals that different physicochemical phenomena sustain the kinetics of membranes fusion depending on whether the diametral area of the vesicle is already exposed ($a > 0.5$) or not ($a < 0.5$).

The topology of the system changes on each side of the diametral plane of the vesicle (Figure 5). Thus, when the diametral plane is not yet uncovered (see cartoon in Figure 5a), the vesicle membrane still encloses partially the vesicle, so that its tension remains high due to the locally refrained swelling of the matrix. This allows to neglect the relatively small edge energy of the rim connecting the vesicle and cell membranes. Thus, progress of fusion results in the release of energy due to the change of membrane tension upon transfer of the tense vesicle membrane lipids into the comparatively relaxed cell membrane ($\sigma_v > \sigma_c$) :

$$(dW_{\text{released}})_{a < 0.5} \approx 2\pi (\sigma_v - \sigma_c)R.dR \quad (2)$$

where R is the radius of the circular rim. In order for the fusion to progress, this energy must be dissipated, so that the rate of fusion is necessarily controlled by its rate of dissipation. Following an analysis proposed by F. Brochard and P.G. de Gennes^[29, 30] for a similar physical situation, we consider that the main dissipation occurs by viscous losses, so that:

$$4\pi\eta R(dR/dt) = W_{\text{released}} \quad (3)$$

where η is the surface viscosity of the cell membrane. Combination of Equations (2) and (3) evidences that the radius of the rim enlarges exponentially as soon as the initial energy of the pore has been dissipated (Figure 5a). After the diametral plane has been uncovered, the matrix can swell freely in any freshly exposed area (see cartoon in Figure 5b) so that, the vesicle membrane tension drops and becomes close to that of the cell. Incorporation of the vesicle membrane into that of the cell occurs then without significant change of surface tension energy. Therefore, a lower energy is released during this second phase and corresponds mostly to that featuring the resorption of the rim created at the junction between the two membranes. Thus :

$$(dW_{\text{released}})_{a > 0.5} = -2\pi\rho^* dR \quad (4)$$

where ρ^* is the coefficient of line energy per unit of length of the rim perimeter. Combination of Equations (3) and (4) predicts that the radius of the rim should decrease linearly with time, a fact which is effectively observed experimentally (Figure 5b).

The intravesicular matrix plays a major role in these dynamics since its constricted swelling provides the

energy which leads to the fusion pore rupture and then maintains the vesicle membrane under tension up to the point where the diametral zone of the vesicle is uncovered. At the end of phase III, the polyelectrolytic matrix has only released 20-30 % of its initial catecholamines content.^[19, 31] Then the rest of neurotransmitter molecules simply progressively diffuse away from the swollen matrix; this corresponds to the tail of the spike.^[14, 31] Thus, in agreement with previous conjectures on secretion without full-fusion, this model indicates that small vesicles should not develop a sufficient pressure for their membrane surface tension to overcome the pore edge resistance. We estimated that the depleted volume into the vesicle at the moment of the pore rupture corresponds approximately to that of a half-sphere containing about 20,000 molecules, *i.e.*, of about 25 nm radius.^[15] Assuming that the energetics of the present adrenal chromaffin vesicles can be extrapolated to other catecholaminergic vesicles, vesicles with radii less than about 25 nm should never reach full fusion and thereby, should release their content only through their stable initial fusion pores. These values correspond to the molecular content and dimensions of many catecholaminergic neuronal vesicles, which are thought to lead mostly to “kiss & run” events, *i.e.*, to fusion pore release only. Conversely, unless another mechanism closes the fusion pore before the rupture point is reached, larger vesicles (such as the dense core vesicles examined here or those of mast cells^[31]) should always release mostly through full fusion since 20,000 molecules represents a very minute fraction of the total amount of catecholamines that they contain (3,000,000 for chromaffin cells).^[4, 14, 19]

The above model has been shown to be consistent with the kinetic data extracted from individual events monitored at chromaffin cells. It shows also that the kinetics of release is tightly controlled by the surface tension of the vesicle and by the viscosity of the cell membrane. We wished therefore to design experiments in order to modify these parameters so as to test these key hypotheses of our model.

A first series of experiments involved the effect of small concentrations of trivalent cations. The exchange of catecholamine cations in the matrix occurs then by these trivalent cations in concurrence with Na⁺ and H⁺ which are present in large excess. Partial incorporation of trivalent cations in the matrix is expected to decrease its swelling since these species provide more interactions with the anionic sites of the gel.^[23, 24] This should reduce the internal pressure inside the vesicle and henceforth decrease the surface tension of the vesicle at the same stage of release. This should therefore increase the stability of the initial fusion pore and thereby, decrease the frequency of full fusion events. Furthermore, a lesser expansion of the matrix is expected to reduce drastically the diffusion coefficient of the catecholamines in the swollen zones of the matrix, so that the current

maxima of the observable spikes should be reduced. Finally, whenever diffusion inside the matrix occurs by percolation, some areas of the matrix may be isolated by local compacting of the domains of matrix due to their local constriction by the trivalent ions, leading to an apparent overall decrease of charge released.

The effect of 0.2 to 10 mM La^{3+} (LaCl_3) solutions was thus tested on the chromaffin cells response (Figure 6) following the procedures described by Marszaleck P.E. et al.^[24] on isolated granules of beige mouse mast cell vesicles. Short-term injections (30 to 60 s) of these solutions on the environment of the cell by a micropipette prevented interferences of La^{3+} ions on other metabolic pathways or additional stimulation of exocytosis.^[32, 33] As soon as the cell was bathed with the La^{3+} solution, we observed a striking decrease of spikes frequency and of the amplitude of the remaining spikes (see the almost complete disappearance of spikes in Figure 6a). This was reversible since secretion was again detected after the lanthanide solution diffused away from the cell (see Figure 6a). These variations were larger as the lanthanide concentration was increased, so that at 10 mM, exocytosis almost stopped (Figure 6b,c). These results are thus in complete agreement with our model predictions.

In a second series of experiments, the role of the vesicle membrane tension and of the cell membrane viscosity were experimentally tested following a protocol similar to that defined above, yet in this case, chromaffin cells were submitted to hyper- or hypoosmotic transient stresses during adrenaline releases.^[35] As evidenced on the photographs shown in Figure 7 the cell contracts rapidly when submitted to a hyperosmotic stress because it loses water to restore its osmotic equilibrium with its environment. This decreases the inner cellular volume so that the cell membrane area becomes too large. This provokes a folding of the cell membrane (see Figure 7a), with the dual consequence that the cell membrane tension drops while its apparent viscosity increases. In agreement with the expected consequences of such variations based on our model, a progressive decrease of the peak frequency was observed (Figure 7a,b). This reduced frequency was maintained as long as the cell remained contracted under hyperosmotic conditions. The mean decrease correlated with the intensity of the hyperosmotic condition, being close to 50 % and 90 % for solutions about 2 and 3 times respectively more concentrated than the isotonic medium (Figure 7b). When the injection of these hyperosmotic solutions was interrupted, isotonic conditions were progressively restored around the cell by diffusion and the cell recovered gradually its initial shape. Simultaneously, the peak frequency increased to return to the level of the control cell responses (isotonic medium). The analysis of the peak characteristics during hyperosmotic injections (at

750mOsm see Figure 7c) versus isotonic conditions (before and after injection) showed that the maximum current of the remaining spikes decreased (about 30 %) while the charge released was almost unaffected. These results are in good agreement with our predictions since a decreased cell membrane tension should delay the moment at which the rupture of the initial fusion pore occurs (eqn. (1)), thereby decreasing the frequency of the full fusion events. For these events where the full fusion stage is still reached, an increase in the cell membrane viscosity is expected to reduce the rate at which the fusion energy may be dissipated (eqn. (2))^[19,29] and henceforth^[31, 34] to reduce the intensity of the observable spikes without affecting significantly the charge released (Figure 7c). This effect on the rate of membrane unfolding is better evidenced through the comparison of the time variations of the fractional area of the vesicle membrane incorporated into the cell membrane between iso- and hyperosmotic conditions [$a(t)$, Figure 7d]. However, none of these osmotic stresses should significantly alter the overall diffusivity in the swollen matrix in agreement with the observations that the total released amount of catecholamines is not significantly affected (Figure 7c). Conversely, in hypoosmotic conditions (data not shown) the water entry in the cell increases the cell inner volume and henceforth the mechanical tension of its membrane and possibly decrease the viscosity of its membrane. This is expected to facilitate the fusion pore rupture and increase the rate of the fusion process. This is precisely what was observed by us (data not shown) and others^[36] since hypoosmotic stresses led to an amplification of the peak frequency and to an increase of the current spike maxima without significant change of the charge released. Therefore, both series of results support qualitatively the basic assumptions of our model.

The two above series of experiments involving La^{3+} ions or hyper-/hypoosmotic stresses allowed us to test experimentally the effect of the key factors, which within our present view of the physicochemical events, control on the one hand the transition between fusion pore release and full fusion, and on the other hand regulate the dynamics of the full fusion stage. In the following third series of experiments, we attempted to modify only the viscosity of the membrane since this should only affect the cell ability to dissipate the energy released during the full fusion and not at all the transition between pore-release and full fusion. For this purpose, the chromaffin cells were incubated with cholesterol during 48 hrs, before release was elicited (Figure 8).^[37, 38] As expected, and in sound contrast with the two above experiments, the frequency of the spikes was not altered. However, we observed that their rise-time as defined by the duration $t_{90\%} - t_{20\%}$ as indicated in Figure 8a, increased on cells incubated with cholesterol (these variations are presented separately for spikes with or without pre-spike feature in Figure 8d and 8c, respectively). This reduced time-rise evidenced that the rate of membrane unfolding was

significantly reduced^[31, 34] in agreement with the lower ability of the cell membrane to dissipate the released energy during each event (eqn. (3)). We also observed that the fraction of pre-spike events increased from about 30% for control cells to 50% for those incubated with cholesterol, and that the mean duration of these pre-spike features was increased significantly (Figure 8b). In fact, often they could not be considered anymore as usual “feet” representative of the fusion pore release. More work is evidently required before being able to account for the occurrence of these special pre-spike events and to describe their kinetics. However, one may tentatively guess that they are related to the cell membrane heterogeneities near the fusion pore which are presumably exacerbated by the cholesterol structuration of the membrane.^[39-41] In this view, full fusion could well proceed then by stages involving sequential areas of the cell membrane with different abilities to dissipate the energy released during the full fusion.

Acknowledgements

This work has been supported in part by CNRS (UMR 8640; Program “*Dynamique et réactivité des assemblages biologiques*”), Ecole Normale Supérieure and by the French Ministry of Research (MDRNT). I.B. acknowledges a PhD fellowship from CONACYT-SFERE, and M.G. acknowledges a PhD fellowship from MDRNT. We are also greatly indebted to the slaughterhouse of Meaux (France) for the supply of adrenal glands and to UPR 1929 (CNRS, Paris) and to its Director, Dr. J.P. Henry, for the chromaffin cells preparation.

References

- [1] D. Bruns, R. Jahn, *Nature* **1995**, 377, 62-65.
- [2] D. Zenisek, J. A. Steyer, W. Almers, *J. Neurochem.* **2001**, 78, 2-2 Suppl. 1.
- [3] J. M. Finnegan, K. Pihel, P. S. Cahill, L. Huang, S. E. Zerby, A. G. Ewing, R. T. Kennedy, R. M. Wightman, *J. Neurochem.* **1996**, 66, 1914-1923.
- [4] T. J. Schroeder, J. A. Jankowski, J. Senyshyn, R. W. Holz, R. M. Wightman, *J Biol. Chem.* **1994**, 269, 17215-17220.
- [5] J. Rizo, T. C. Sudhof, *Nat. Struct. Biol.* **1998**, 5, 839-842.
- [6] S. J. Cho, M. Kelly, K. T. Rognlien, J. A. Cho, H. Heinrich, B. P. Jena, *Biophys. J.* **2002**, 83, 2522-2527.
- [7] Y. Humeau, F. Doussau, N. J. Grant, B. Poulain, *Biochimie* **2000**, 82, 427-446.
- [8] L. J. Breckenridge, W. Almers, *Nature* **1987**, 328, 814-817.
- [9] A. Albillos, G. Dernick, H. Horstmann, W. Almers, G. A. deToledo, M. Lindau, *Nature* **1997**, 389, 509-512.
- [10] J. Zimmerberg, M. Curran, M. Brodwick, F. S. Cohen, *Biophys. J.* **1987**, 51, A357-A357.
- [11] G. A. de Toledo, R. Fernandez Chacon, J. M. Fernandez, *Nature* **1993**, 363, 554-558.
- [12] L. M. Johns, E. S. Levitan, E. A. Shelden, R. W. Holz, D. Axelrod, *J. Cell Biol.* **2001**, 153, 177-190.
- [13] D. Zenisek, J. A. Steyer, W. Almers, *Nature* **2000**, 406, 849-854.
- [14] C. Amatore, Y. Bouret, L. Midrier, *Chem-Eur. J.* **1999**, 5, 2151-2162.
- [15] C. Amatore, Y. Bouret, E. R. Travis, R. M. Wightman, *Angew. Chem. Int. Edit.* **2000**, 39, 1952-1955.
- [16] C. Amatore, S. Arbault, D. Bruce, P. de Oliveira, M. Erard, M. Vuillaume, *Faraday Discuss.* **2000**, 319-333.
- [17] S. F. Dressman, J. L. Peters, A. C. Michael, *J. Neurosci. Meth.* **2002**, 119, 75-81.
- [18] K. Pihel, T. J. Schroeder, R. M. Wightman, *Anal. Chem.* **1994**, 66, 4532-4537.
- [19] C. Amatore, Y. Bouret, E. R. Travis, R. M. Wightman, *Biochimie* **2000**, 82, 481-496.
- [20] J. A. Jankowski, T. J. Schroeder, E. L. Ciolkowski, R. M. Wightman, *J. Biol. Chem.* **1993**, 268, 14694-14700.
- [21] A. J. Daniels, R. J. P. Williams, P. E. Wright, *Neuroscience* **1978**, 3, 573-585.
- [22] R. Borges, J. D. Machado, C. Alonso, M. A. Brioso, J. F. Gomez, in *Chromogranins: Functional and Clinical Aspects*, Vol. 482, **2000**, pp. 69-81.

- [23] M. J. Curran, M. S. Brodwick, *J. Gen. Physiol.* **1991**, *98*, 771-790.
- [24] P. E. Marszalek, B. Farrell, P. Verdugo, J. M. Fernandez, *Biophys. J.* **1997**, *73*, 1169-1183.
- [25] J. R. Monck, J. M. Fernandez, *Curr. Opin. Cell Biol.* **1996**, *8*, 524-533.
- [26] W. Almers, *Nature* **2001**, *409*, 567-568.
- [27] A. Chanturiya, L. V. Chernomordik, J. Zimmerberg, *P. Natl. Acad. Sci. U.S.A.* **1997**, *94*, 14423-14428.
- [28] T. J. Schroeder, R. Borges, J. M. Finnegan, K. Pihel, C. Amatore, R. M. Wightman, *Biophys. J.* **1996**, *70*, 1061-1068.
- [29] O. Sandre, L. Moreaux, F. Brochard-Wyart, *P. Natl. Acad. Sci. U.S.A.* **1999**, *96*, 10591-10596.
- [30] P.G. de Gennes, *Rev. Mod. Phys.* **1985**, *57*, 827-862.
- [31] B. Farrell, S. J. Cox, *B. Math. Biol.* **2002**, *64*, 979-1010.
- [32] P. D. Marley, P. J. R. Bales, M. Zerbes, D. A. Powis, M. O'Farrell, *J. Neurochem.* **2000**, *75*, 1162-1171.
- [33] D. A. Powis, C. L. Clark, *Neurosci. Lett.* **1996**, *203*, 131-134.
- [34] C. Amatore, L. Midrier, *unpublished results*. L. Midrier DEA University Pierre et Marie Curie (Paris, France), June 1996.
- [35] K. P. Troyer, R. M. Wightman, *J. Biol. Chem.* **2002**, *277*, 29101-29107.
- [36] R. Borges, E. R. Travis, S. E. Hochstetler, R. M. Wightman, *J. Biol. Chem.* **1997**, *272*, 8325-8331.
- [37] V. Bolotina, V. Omelyanenko, B. Heyes, U. Ryan, P. Bregestovski, *Pflug. Arch. Eur. J. Phys.* **1989**, *415*, 262-268.
- [38] J. A. Lundbaek, P. Birn, J. Girshman, A. J. Hansen, O. S. Andersen, *Biochem.* **1996**, *35*, 3825-3830.
- [39] T. Lang, D. Bruns, D. Wenzel, D. Riedel, P. Holroyd, C. Thiele, R. Jahn, *Embo J.* **2001**, *20*, 2202-2213.
- [40] E. Ikonen, *Curr. Opin. Cell Biol.* **2001**, *13*, 470-477.
- [41] W. B. Huttner, J. Zimmerberg, *Curr. Opin. Cell Biol.* **2001**, *13*, 478-484.
- [42] R. M. Wightman, J. A. Jankowski, R. T. Kennedy, K. T. Kawagoe, T. J. Schroeder, D. J. Leszczyszyn, J. A. Near, E. J. Diliberto, O. H. Viveros, *P. Natl. Acad. Sci. U.S.A.* **1991**, *88*, 10754-10758.

Figure Captions

Figure 1.

Cartoon of a neuronal chemical synapse. Neurotransmitter molecules are stored into vesicles located at the terminal junction of the emitting neuron. Stimulation of this neuron leads to the influx of Ca^{2+} through specific pumps located in its terminal zone, which provokes the docking of vesicles to the pre-synaptic membrane. Neurotransmitters are then released in the very narrow synaptic cleft and detected by specific receptors, located on the post-synaptic membrane of the receiving neuron. This transmission of chemical messengers induces the propagation of the nerve information from the emitting neuron to the receiving one.

Figure 2.

Schematic representation of the main phases of exocytosis during full fusion of dense core vesicles with cell membrane. Following the cell stimulation (calcium influx), some vesicles are primed to effect exocytosis (*I*) and dock to the cell membrane. After the formation of a fusion pore, catecholamine neurotransmitters begin to diffuse out of the vesicular matrix through the pore (*II*). The continuous exchange of catecholamine cations with external cations such as Na^+ and H^+ during phase *II* diminishes the cohesion of the matrix, which increases the surface tension of the vesicle membrane. When this tension becomes high enough to disrupt the fusion pore structure, full fusion of the vesicle and cell membranes occurs resulting in the incorporation of the vesicle membrane into that of the cell (*III*). This process pursues up to the point where the vesicular matrix is fully exposed to the extracellular fluid (*IV*).

Figure 3.

(a) Cartoon of an “artificial synapse” (top) and actual microscopic view (bottom) showing a carbon fiber ultramicroelectrodes (black) placed into contact with a chromaffin cell (disc in the center) stimulated by a barium ion solution injected through a micropipette (white, in the right bottom quadrant of the view). (b) Series of single vesicular events observed through amperometric oxidation of adrenaline molecules (2 e/molecule at $E=+650\text{ mV vs. Ag/AgCl}$).^[42] A typical spike extracted from the trace (b) is enlarged in (c) with a sketch showing a pre-spike feature (as observed on about 30% of the amperometric events; see Figure 8a) evidencing release through the initial fusion pore. In (c), the different phases of the exocytosis defined in Figure 2 are identified by their labels (*I-IV*).

Figure 4.

Series of three typical experimental amperometric spikes ($i(t)$, peaked solid curves) normalized versus their maximum current and compared to the current variations predicted through the model discussed here (open circles). In each case, the resulting time-course of the function $a(t)$, which represents the fraction of the vesicular membrane already incorporated into the cell membrane, is also represented (open triangles). Insets: enlargement of the variations of $a(t)$ at short times. Release was elicited with injection of BaCl_2 2mM in Locke buffer supplemented with 0.7 mM MgCl_2 , without carbonates.

Figure 5.

Time variations of R/R_{vesicle} , *i.e.*, of the radius of the rim connecting the cell and vesicle membranes (see cartoons) normalized to that of the vesicle. This is represented separately in (a) for the first half ($a(t) < 0.5$) and second half (b: $a(t) > 0.5$) of the full fusion process. In (a),^[14] three representative events (symbols) are overlaid over a set of theoretical variations predicted based on Equations (2, 3) considering different initial energies at the very beginning of phase *III*. (b)^[14] Unified presentation of the variations of the pore radius during the final stage of full fusion (t_x is the time at which $a(t_x) = x$). The linear variation with time (correlation coefficient: 0.998; 596 events are shown) agrees with the predictions of the model presented here (eqns. 3 and 4).

Figure 6.

Effect of lanthanide ions injection (0.3 to 10 mM LaCl_3 in Locke buffer supplemented with 0.7 mM MgCl_2 , without carbonates) on the release of adrenaline by chromaffin cells. Cell secretion was first elicited by a 10 s barium solution (BaCl_2 2mM in Locke buffer supplemented with 0.7 mM MgCl_2 , without carbonates); The ultramicroelectrode was then placed into contact with the cell membrane to monitor release and the micropipette was replaced by another one containing the lanthanide ions solution (10 mM La^{3+} for the traces shown in (a)), which was injected onto the cell during 60 s (see marker in (a)). The frequency (b), maximum current (c) and charge (c) of the spikes measured during the phase of lanthanide ions injection are represented as their mean values (\pm S.D.) relative to those determined before and after the injection of lanthanide ions (for measurements after, a delay of 60 s was allowed to let La^{3+} completely diffuse away from the cell).

Figure 7.

Effect of transient exposures (30 to 60 s) to hyperosmotic media (630, 750 or 970 mOsm obtained by adjusting

the NaCl concentration of Locke buffer supplemented with 0.7 mM MgCl₂, without carbonates) on adrenaline release by chromaffin cells. The experiments were conducted as for the stimulation by La³⁺ in Figure 6, except that the second micropipette contained the hyperosmotic solution (970 mOsm for the traces shown in (a)). The cell shape (pictures 1 to 3 in (a)) was observed in parallel with a video camera mounted on the microscope. The spikes frequency variations are reported in (b) as a function of the time-course of the experiment for different hyperosmotic solutions (see numbers in mOsm on each curve). The mean (\pm S.D.) values of the maximum current and total charge of the spikes during the 30 s-long period where the effect of the hyperosmotic medium was maximum, are compared in (c) for the isotonic (*Iso* at 315 mOsm.) and hyperosmotic (*Hyper*: 750 mOsm) conditions. In (d) the corresponding mean variations of the function $a(t)$ are represented for the isotonic (*Iso* at 315 mOsm.) and hyperosmotic (*Hyper*: 750 mOsm) conditions.

Figure 8.

Effect of cholesterol (incubation: 48 H. at 0.25 mM in buffer supplemented with 10 % Fetal Calf Serum)^[37] on release of adrenaline by chromaffin cells. (a) Typical amperometric spike showing a pre-spike feature and the definition of the parameters reported in (b)-(d). (b) Mean duration of the clearly observable pre-spike features (occurring for about 30% of spikes under control conditions (*CTR.*) and for about 50% of spikes for cholesterol incubated cells (*CHS.*)). (c,d) Comparison of the mean rise-time $t_{90\%}-t_{20\%}$, (defined in (a)) for the spikes displaying (c) or not (d) a clearly observable pre-spike feature.

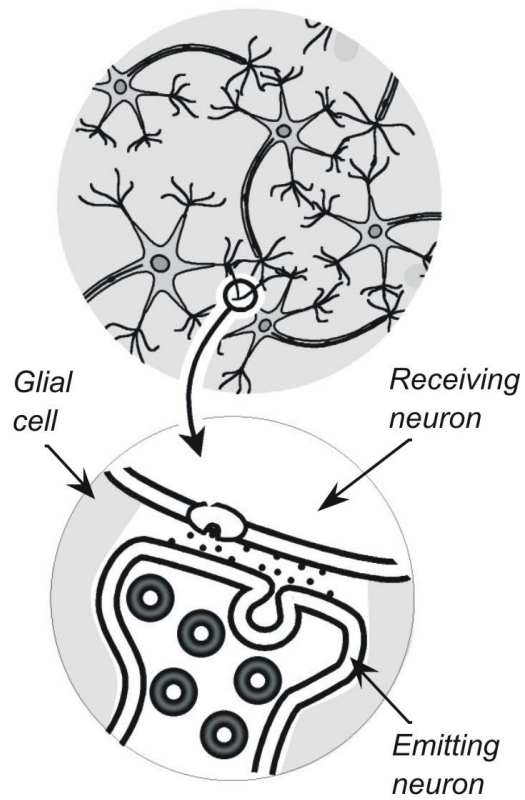


Figure 1

Dynamics of Full Fusion During Vesicular Exocytotic Events: Release of Adrenaline by Chromaffin Cells.

Christian Amatore,* Stéphane Arbault, Imelda Bonifas, Yann Bourret, Marie Erard and Manon Guille.

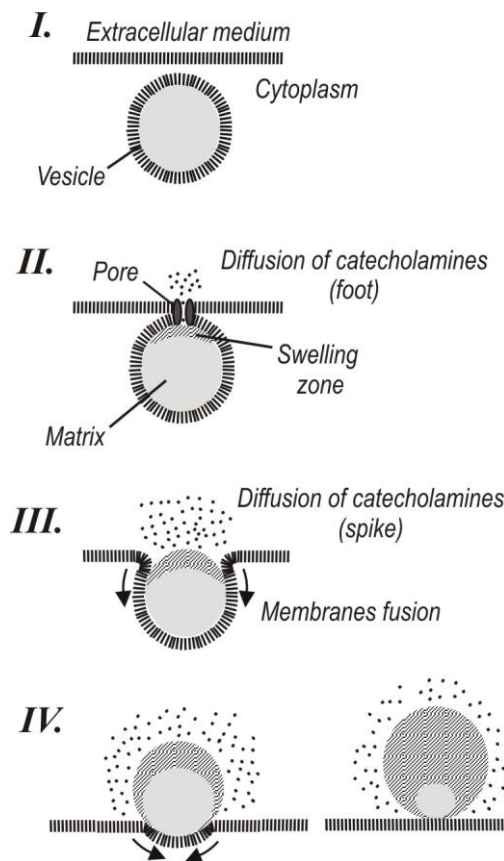


Figure 2

Dynamics of Full Fusion During Vesicular Exocytotic Events: Release of Adrenaline by Chromaffin Cells.

Christian Amatore,* Stéphane Arbault, Imelda Bonifas, Yann Bourret, Marie Erard and Manon Guille.

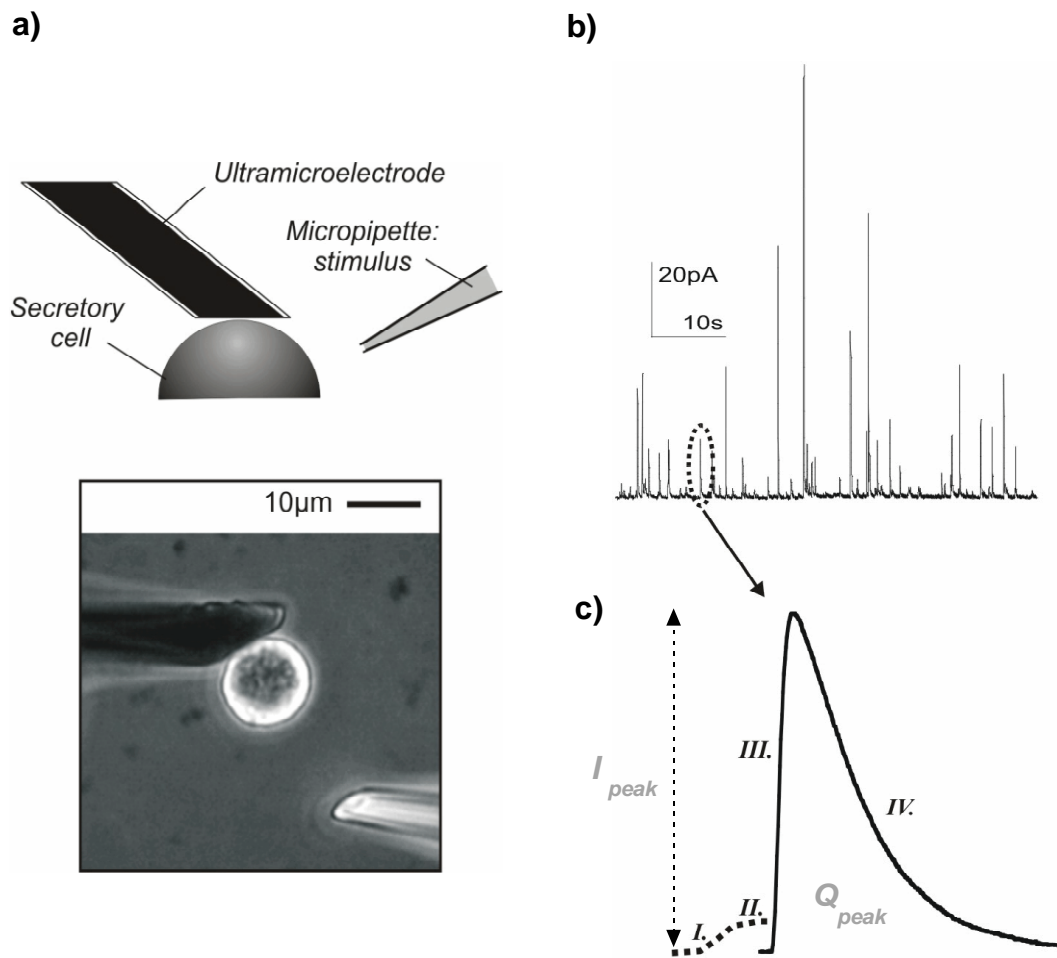


Figure 3

Dynamics of Full Fusion During Vesicular Exocytotic Events: Release of Adrenaline by Chromaffin Cells.

Christian Amatore,* Stéphane Arbault, Imelda Bonifas, Yann Bourret, Marie Erard and Manon Guille.

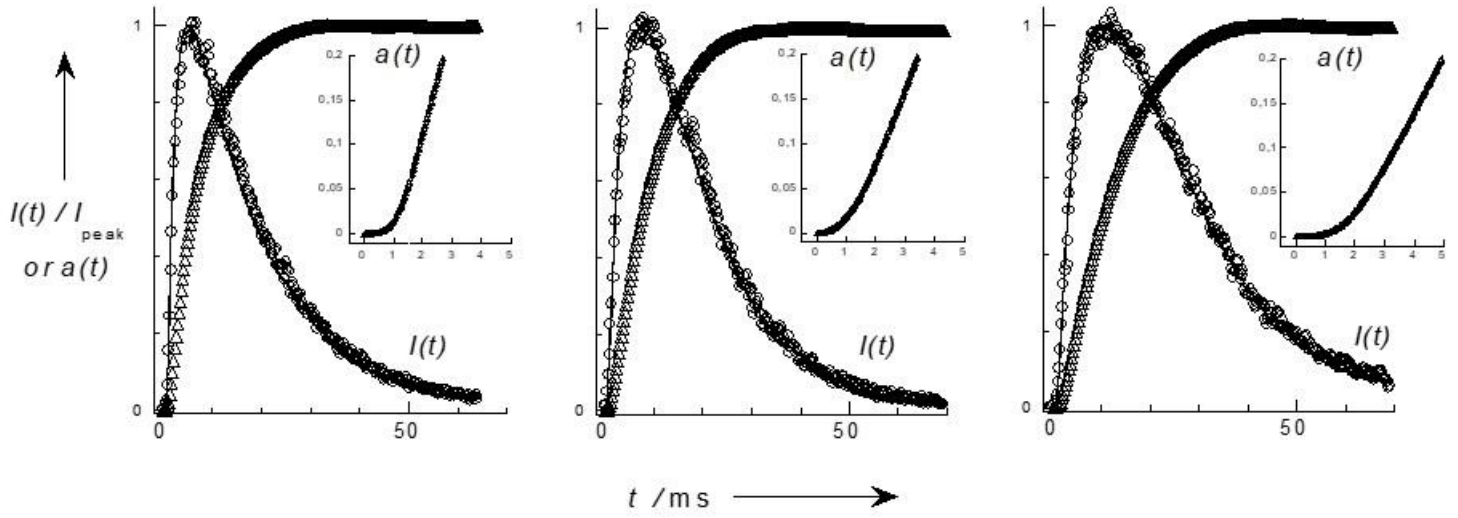


Figure 4

Dynamics of Full Fusion During Vesicular Exocytotic Events: Release of Adrenaline by Chromaffin Cells.

Christian Amatore,* Stéphane Arbault, Imelda Bonifas, Yann Bourret, Marie Erard and Manon Guille.

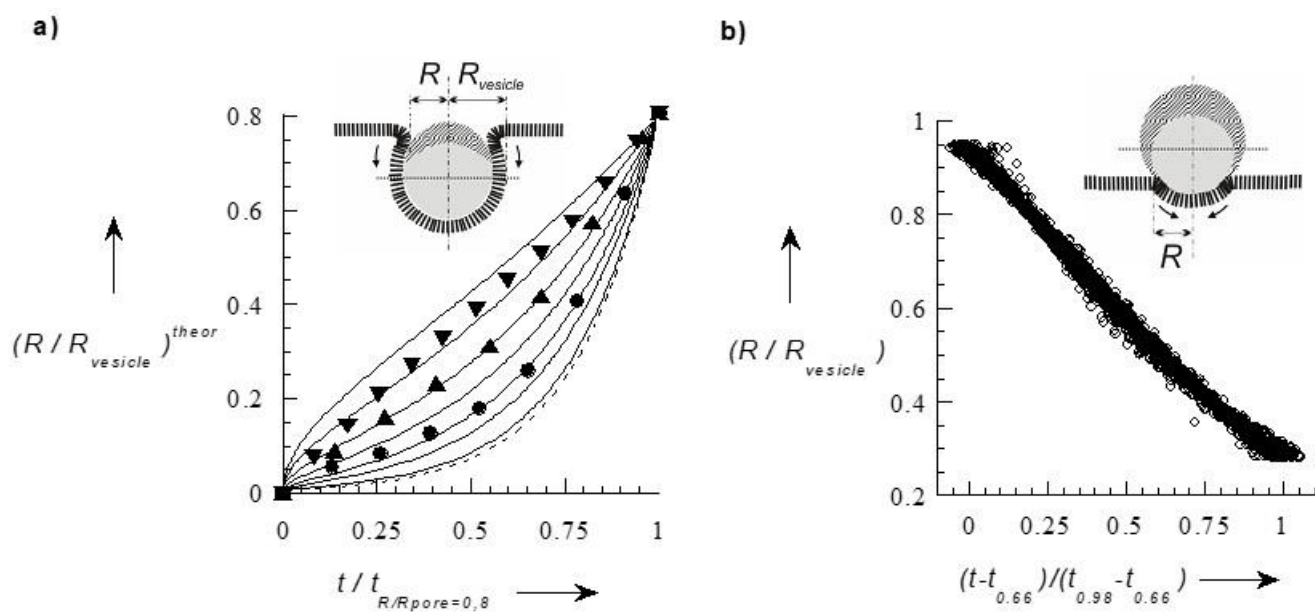


Figure 5

Dynamics of Full Fusion During Vesicular Exocytotic Events: Release of Adrenaline by Chromaffin Cells.

Christian Amatore,* Stéphane Arbault, Imelda Bonifas, Yann Bourret, Marie Erard and Manon Guille.

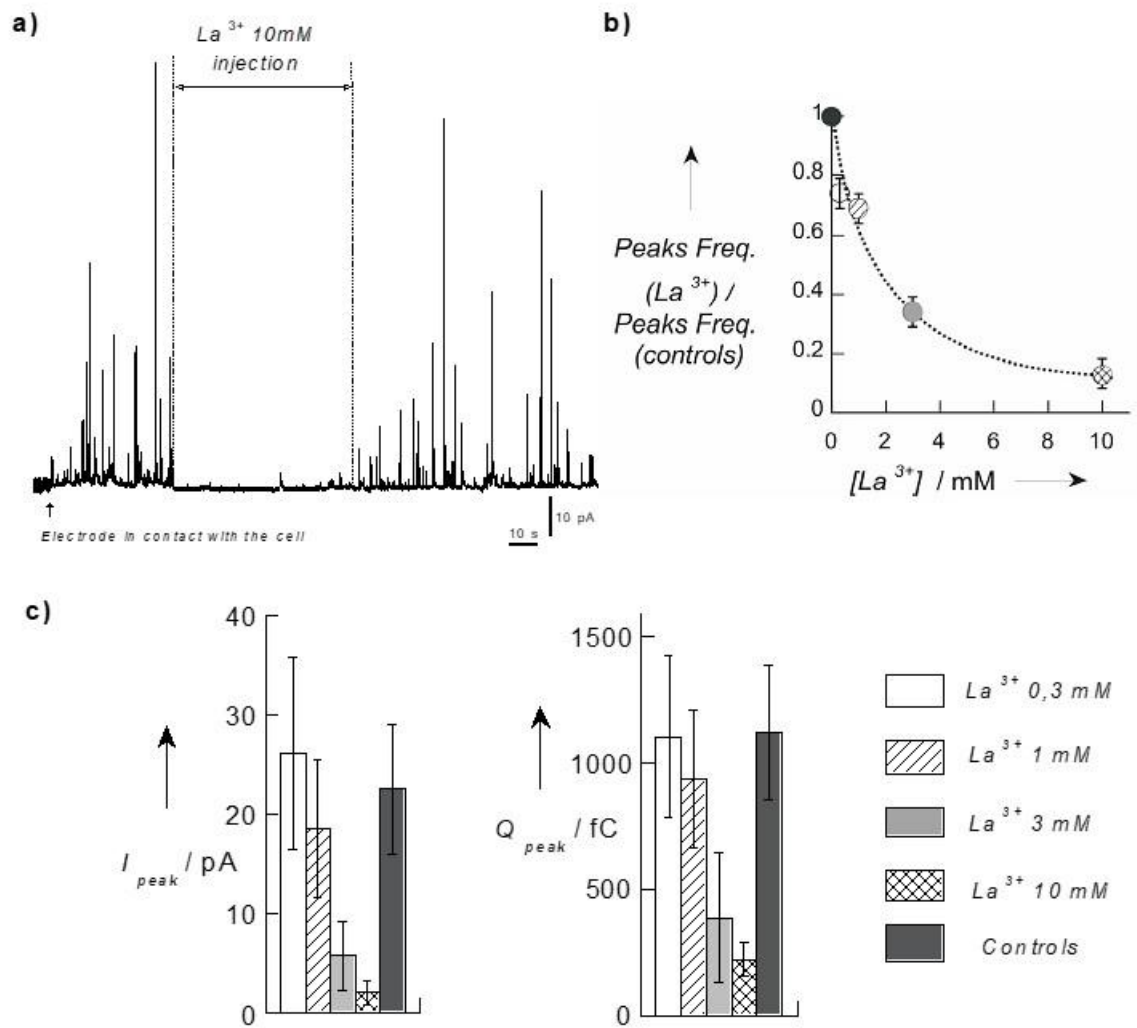


Figure 6

Dynamics of Full Fusion During Vesicular Exocytotic Events: Release of Adrenaline by Chromaffin Cells.

Christian Amatore,* Stéphane Arbault, Imelda Bonifas, Yann Bourret, Marie Erard and Manon Guille.

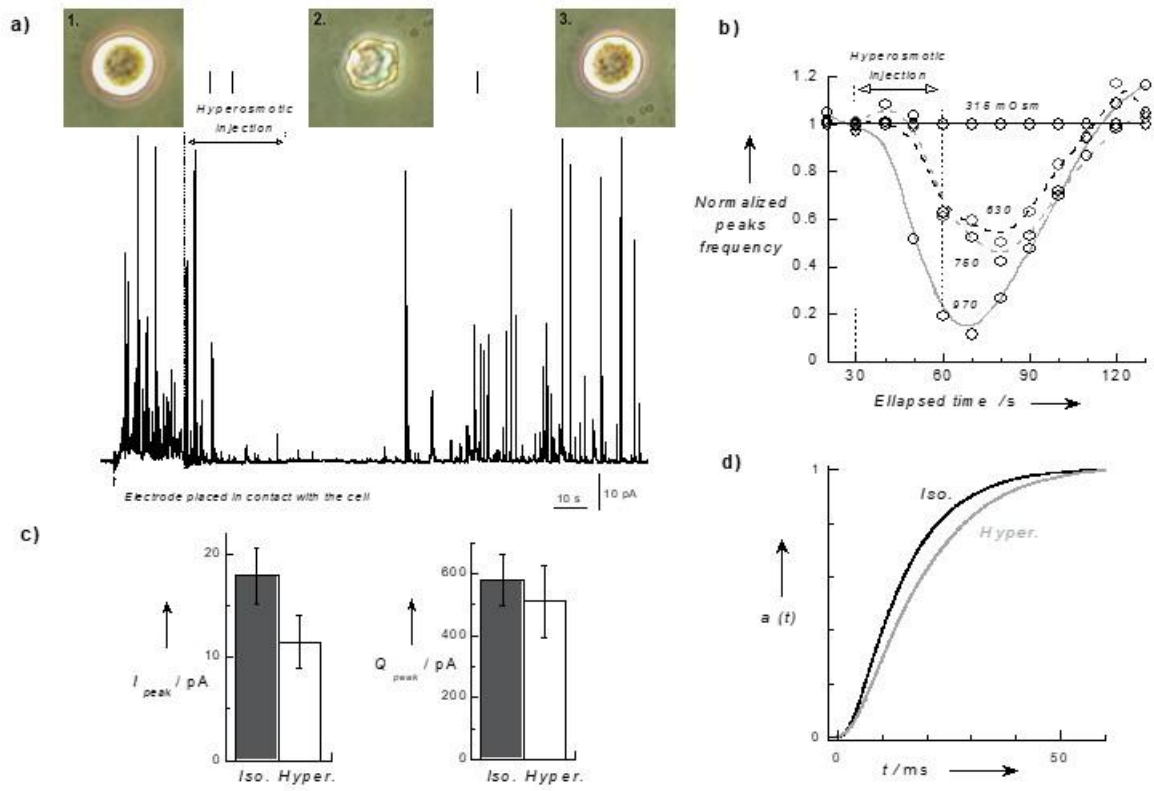


Figure 7

Dynamics of Full Fusion During Vesicular Exocytotic Events: Release of Adrenaline by Chromaffin Cells.

Christian Amatore,* Stéphane Arbault, Imelda Bonifas, Yann Bourret, Marie Erard and Manon Guille.

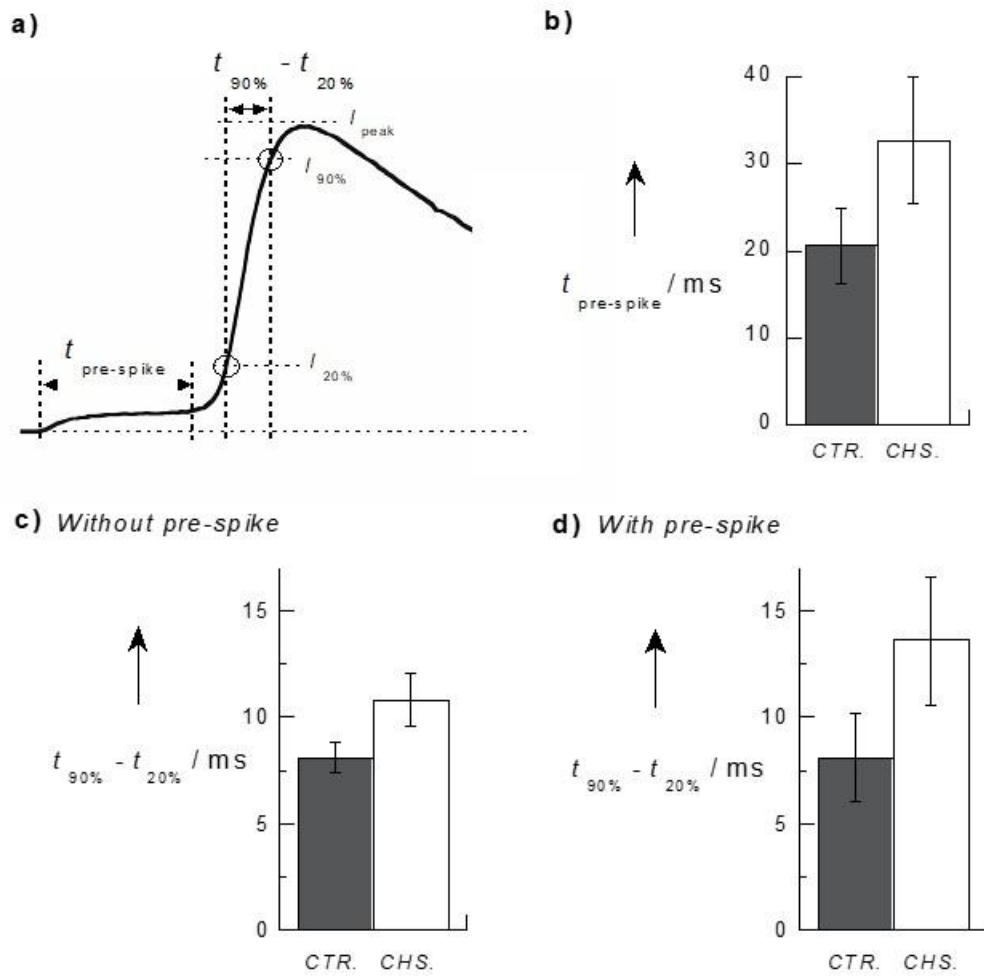


Figure 8

Dynamics of Full Fusion During Vesicular Exocytotic Events: Release of Adrenaline by Chromaffin Cells.

Christian Amatore,* Stéphane Arbault, Imelda Bonifas, Yann Bourret, Marie Erard and Manon Guille.